Applied Surface Science 265 (2013) 553–557

Contents lists available at SciVerse ScienceDirect

Applied Surface Science

journal homepage: www.elsevier.com/locate/apsusc

Morphology evolution of *a*-plane ZnO films on *r*-plane sapphire with growth by pulsed laser deposition

Chun-Yen Peng*, Jr-Sheng Tian, Wei-Lin Wang, Yen-Teng Ho, Li Chang

Department of Materials Science and Engineering, National Chiao Tung University, Hsinchu, Taiwan, ROC

ARTICLE INFO

Article history:
Received 5 October 2012
Received in revised form 6 November 2012
Accepted 12 November 2012
Available online 23 November 2012

Keywords:
ZnO
Morphology
Epitaxial growth

ABSTRACT

In this study, the morphology evolution of epitaxial *a*-plane ZnO on *r*-plane sapphire at low and high temperatures with growth by pulsed laser deposition (PLD) are presented. Examination of the surfaces of ZnO films during growth was done with in situ reflection high energy electron diffraction, and atomic force microscopy was used to examine the surface morphology of the corresponding films after growth. For initial growth, it was observed that (1×2) reconstruction on ZnO grown at 750 °C (HT-ZnO) occurred with step-flow growth, while ZnO grown at 450 °C (LT-ZnO) exhibited island growth mode. For thick films both HT- and LT-ZnO surfaces eventually develop into stripe morphology. Significant change of surface morphology during cooling had also been observed.

© 2012 Elsevier B.V. All rights reserved.

1. Introduction

As a wide direct bandgap wurtzite semiconductor, zinc oxide (ZnO) is an attractive material for potential applications in optoelectronic devices, such as light emitting devices [1–4], transparent thin-film transistors [5,6], transparent electrodes [7–9], and solar cells [10–12]. Recently, growth of nonpolar ZnO epitaxial films has attracted a lot of interest due to the lack of the red-shift caused by quantum confined Stark effect [13–21]. Because the spontaneous polarization of ZnO is nearly two times of GaN ($-0.057\,C/m^2$ versus $-0.029\,C/m^2$) [22], ZnO films without polarity along the growth direction are important for light emitting applications.

R-plane sapphire substrate is one of commonly used substrates for growth of epitaxial *a*-plane nonpolar thin films of GaN and ZnO. Nonpolar *a*-plane ZnO epitaxial films grown on it have been achieved by domain matching epitaxy method [23] using pulsed laser deposition (PLD) [24], sputtering [25], plasma-assisted molecular beam epitaxy (PAMBE) [26,27], and metal-organic chemical vapor deposition (MOCVD) [28].

Stripe morphologies are the most usually observed feature for nonpolar *a*-plane ZnO epitaxial films. However, Lee et al. have reported Volmer–Weber growth mode for *a*-plane ZnO grown on *r*-plane sapphire by PAMBE at 700 °C [29,30]. In contrast, Chauveau et al. in their study of MBE-grown *a*-plane ZnO on *r*-plane sapphire at 400 °C suggest that the initial growth is not 3D [31]. Though growth of *a*-plane ZnO on *r*-sapphire has been reported by many studies, the evolution of structural properties and surface morphologies with film growth has been incomplete, and the exact related mechanisms are not fully understood.

Reflection high energy electron diffraction (RHEED) is a powerful tool to characterize the surface in situ during film growth. Though it has been used to study *a*-plane ZnO film growth [32–34], the evolution of surface morphology has not yet been reported in details for growth at different temperature. Growing a smooth, low defect density *a*-plane ZnO film is still a challenge for the application of devices. Knowing the evolution of surface morphology is helpful for better understanding of the mechanism for the nucleation and growth with film properties. As a result, an improvement of film quality of *a*-plane ZnO may be realized.

It is known that growth temperature may have a strong effect on crystallinities and optical properties [25,27,35]. In our previous study, we have shown that film growth transition may occur at 600 °C for *a*-plane ZnO formed on *r*-plane sapphire [35]. In this paper, evolution of surface morphologies with film thickness at different growth temperature is studied by employing in situ RHEED to understand what exactly happens during growth. Also, the morphologies after growth have been characterized by atomic force microscopy (AFM) for comparison.

2. Experiments

ZnO film growth on 8 mm × 8 mm *r*-plane sapphire wafers was done by pulsed laser deposition in a Pascal laser-MBE system equipped with a high pressure reflection high energy electron diffractometer (RHEED). The KrF excimer laser irradiation with the

* Corresponding author.
E-mail addresses: cypeng.mse94g@nctu.edu.tw (C.-Y. Peng), lichang@cc.nctu.edu.tw (L. Chang).

0169-4332/$ – see front matter © 2012 Elsevier B.V. All rights reserved.
http://dx.doi.org/10.1016/j.apsusc.2012.11.044

energy density of about 1–3 J/cm^2 and the repetition rate of 2 Hz was used to ablate a sintered ZnO target. Sapphire substrates were ultrasonically cleaned in acetone before loading into the vacuum chamber. Before PLD growth, the substrate was thermally cleaned at 850 °C in vacuum of about 10^{-6} Torr for 30 min. Our previous study of ZnO growth on *r*-plane sapphire at temperatures from 350 to 850 °C has shown that there is a significant difference in growth rate and surface morphology for growth temperature above and below 600 °C [35]. For further study of evolution of surface morphology with film thickness at different temperature in this work, 450 °C (LT-ZnO) and 750 °C (HT-ZnO) were chosen for PLD growth with various number of pulses. Because a high cooling rate can result in significant change on morphological and structural properties [36], the cooling rate was fixed to 30 °C/min for all samples in this work.

Film surface morphologies were in situ examined with high pressure reflection high energy electron diffraction with O_2 ambient at 10^{-2} Torr during growth and cooling. During operation of the RHEED, a double differential pumping unit allowed a vacuum better than 10^{-6} Torr maintain in the electron source while the oxygen pressure in the deposition chamber could be as high as 0.3 Torr. The RHHED patterns were acquired with the electron gun operated at 20 keV and <5° for the incident beam energy and angle, respectively. Atomic force microscopy (AFM) examination was carried out in air after deposition using a Veeco Dimension 5000 scanning probe microscope with a silicon tip (radius of curvature <10 nm) operated in tapping mode. AFM examinations for all the samples were performed within 24 h after PLD growth.

3. Results and discussion

Surface morphological evolution of HT-ZnO and LT-ZnO films on sapphires can be observed by employing in situ RHEED (at growth temperature) and ex situ AFM measurements (at room temperature) as shown in Figs. 1 and 2 where AFM images are on the left column, and RHEED patterns along $[0\,0\,0\,1]_{ZnO}//[\bar{1}\,0\,1\,\bar{1}]_{sapphire}$ and $[\bar{1}\,1\,0\,0]_{ZnO}//[1\,\bar{2}\,1\,0]_{sapphire}$ azimuth, respectively, on the middle and right ones. For evaluation of the cooling effect, room temperature RHEED patterns are included for comparison. For those ZnO deposited with a small number of pulses, the exact film thickness cannot be accurately measured, so we will use the number of pulses to indicate growth in the following unless the film thickness can be determined without significant error by X-ray reflectivity and scanning electron microscopy observation in cross section.

In Fig. 1, the evolution of surface morphologies of ZnO grown at 750 °C with film deposition is evident. Fig. 1(a) shows a typical AFM image of the sapphire substrate after 850 °C thermal cleaning that the surface morphology is step-like with the measured step height of ∼0.3 nm close to interplanar spacing of 0.348 nm for sapphire *r*-plane and an average width of about 250 nm for terraces (roughness ∼0.1 nm). Kikuchi lines on the RHEED pattern (acquired at 750 °C) in Fig. 1(a) also indicate atomically smooth surface on the sapphire. For the initial growth of 50-pulse (<1 nm) HT-ZnO on *r*-plane sapphire, the surface exhibits step morphology (Fig. 1(b)) with ∼80 nm terrace width and ∼0.16 nm step height as measured from the line profile across the step in Fig. 1(b) which is approximate to ZnO *a*-plane d-spacing of 0.163 nm. The roughness of each terrace is below than ∼0.1 nm in average. The corresponding RHEED patterns in $[0\,0\,0\,1]_{Zno}$ and $[1\,\bar{1}\,0\,0]_{ZnO}$ azimuth show streaky lines, suggesting step-flow growth in the very early stage of HT-ZnO film formation at 750 °C. It is interesting to notice that the sharp features in the $[0\,0\,0\,1]_{Zno}$ RHEED pattern change to vaguely spotty reflections after cooling to room temperature (RT), suggesting that thermal stress may modify the surface morphology of *a*-plane ZnO film. It is also noticed that there are additional reflections in $[1\,\bar{1}\,0\,0]_{ZnO}$ pattern, implying that (1×2) reconstruction occurs with step-flow growth [37]. For 200-pulse HT-ZnO deposition on sapphire, the AFM image shows that the step morphology disappears and no clear features can be seen, implying that the surface is totally covered with ZnO islands in ∼20 nm size as evidenced with spotty ZnO reflections in the corresponding RHEED patterns. As the surface roughness of the 200-pulse ZnO is 0.13 nm, the growth mode might change to two-dimensional (2D) nucleation after ZnO film continuously covers the substrate surface. Similar features but with rougher surface morphologies were also observed for >1200-pulse HT-ZnO (roughness 0.3 nm). Also, the grains had grown to ∼30 nm size for 2400-pulse deposited ZnO. The reflection spots were gradually evolving to streaky lines as shown in the RHEED patterns of Fig. 1(d) for ZnO deposition on sapphire up to 4000 pulses, implying that the surface becomes smooth. However, the streaky lines were shortened into spots during cooling to room temperature. AFM measurements show that the surface roughness of 4000-pulse HT-ZnO increases to about 0.38 nm, the grain size increases to ∼30 nm width and 0.3–1.5 nm height. Also, the grains are seen to exhibit more square-like morphology. Significant evolution is further observed on 12000-pulse (∼50–80 nm) HT-ZnO film, as AFM and RHEED in Fig. 1(e) shows a terrace-like morphology with step heights in the range of 0.3–0.9 nm. However, rough steps are seen at terrace edges with protrusions in ∼30 nm width. Though formation of terrace in this stage is not clear, it may evolve from coalescence of square grains in Fig. 1(d). Also, on the 12000-pulse HT-ZnO the surface roughness measured from 1 μm × 1 μm scan area is ∼0.4 nm, and the average roughness on individual terraces is 0.13 nm, similar to that of 200-pulse and 4000-pulse HT-ZnO films. In addition, streaky reflection lines are observed in the RHEED pattern viewed along $[0\,0\,0\,1]_{Zno}$ azimuth at 750 °C, while no apparent change has been observed in $[1\,\bar{1}\,0\,0]_{ZnO}$ azimuth one from the 4000 pulses pattern. For growth to >150 nm films, HT-ZnO evolves to commonly observed stripe morphology with 0.41 nm roughness shown in Fig. 1(f). Such stripes are ∼30 nm wide with 0.3–0.6 nm height difference, which are likely formed from the protrusions in Fig. 1(e) parallel to ZnO *c*-direction along which surface diffusion is known to be fast. Clear streaks are seen in the in situ RHEED pattern along $[0\,0\,0\,1]_{Zno}$ azimuth; however, they change to spots in the RT pattern. It is likely that the film surface with stripes is atomically smooth at HT deposition, and the thermal stress caused by cooling results in undulated stripes.

For low-temperature growth of ZnO on *r*-plane sapphire, the evolution is not the same as for HT ZnO in the initial stage. The AFM image in Fig. 2(a) shows island-like morphology after ZnO deposition of 25 pulses. The islands have widths in 20–50 nm and heights in 0.3–0.6 nm. The measured surface roughness is about 0.17 nm, suggesting that a smooth surface consists of a high density of islands. Therefore, it is likely that 2D nucleation occurs for initial ZnO growth on sapphire. However, the RHEED patterns in Fig. 2(a) clearly show no apparent difference from substrate reflections. For further deposition to 100 pulses, ZnO reflections are clearly seen on the RHEED patterns in Fig. 2(b) similar to those seen in Fig. 1(c) for HT-ZnO. The AFM in Fig. 2(b) shows that the surface is covered with 20–30 nm grains, and the measured surface roughness is ∼0.3 nm. For deposition up to 1200 pulses (∼30 nm thickness), the grain size increases to 40–100 nm length along ZnO *c*-direction with width in 20–30 nm as shown in Fig. 2(c). Also, spots show more pronounced streaks in both $[0\,0\,0\,1]_{Zno}$ and $[1\,\bar{1}\,0\,0]_{ZnO}$ azimuth RHEED patterns but without extra reflections. It is also observed that cooling of LT-ZnO films to room temperature results in the appearance of spotty reflections. Indeed, such shortening of streaks was directly observed even during cooling from 300 to 200 °C, independent of cooling rate of 1–100 °C/min, for both HT- and LT-ZnO

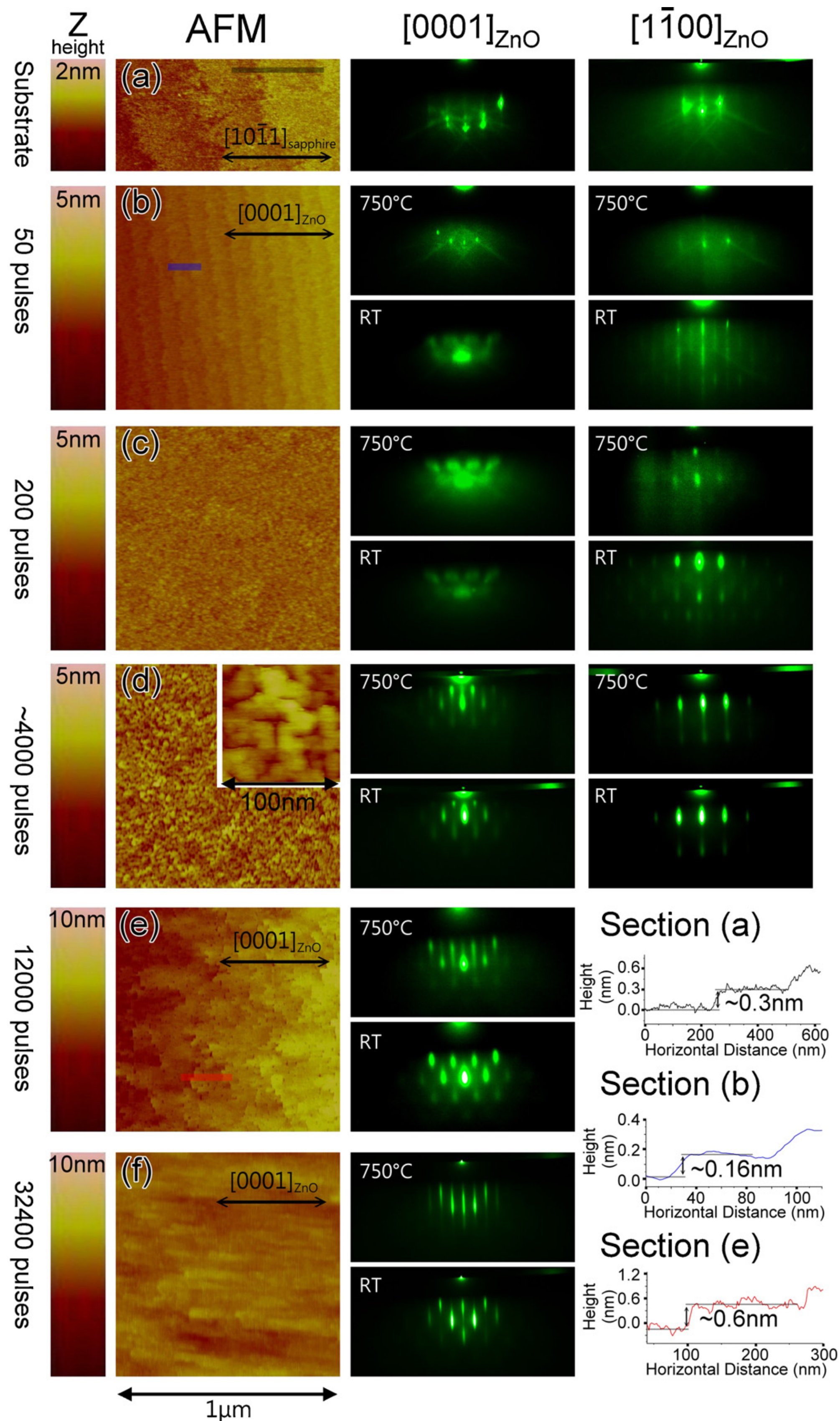

Fig. 1. (Color online) AFM images and RHEED patterns taken from (a) *r*-plane sapphire substrate, and (b) 50 pulses, (c) 200 pulses, (d) 4000 pulses, (e) ~50 nm and (f) ~180 nm HT-ZnO deposited on it. RHEED patterns on the left- and right-hand sides were taken with electron beam incident along $[0\,0\,0\,1]_{Zno}$ and $[1\,\bar{1}\,0\,0]_{ZnO}$, respectively. The patterns of sapphire were taken at 750 °C after thermal cleaning. The upper RHEED patterns in (b)–(f) were in situ taken at growth temperature, and lower ones were taken after cooling to room temperature in the PLD chamber. The line profiles shown in the bottom right corner are plotted from AFM images in (a), (b), and (e). (For interpretation of the reference to color in this figure legend, the reader is referred to the web version of this article.)

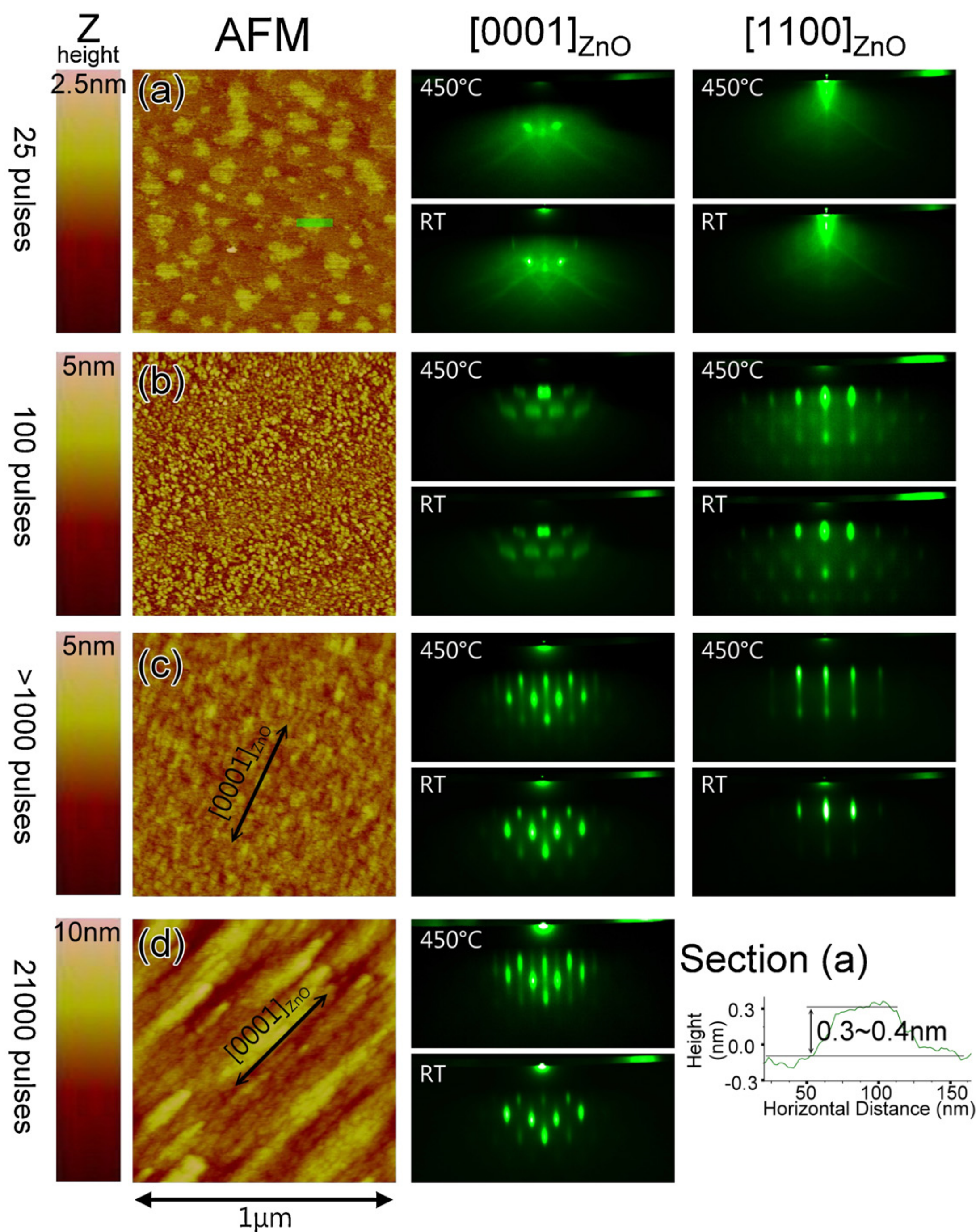

Fig. 2. AFM images and RHEED patterns taken from (a) 25 pulses, (b) 100 pulses, (c) 28 nm (1200 pulses), and (d) ~180 nm ZnO deposited on *r*-plane sapphire at 450 °C. RHEED patterns on the left- and right-hand sides were taken with electron beam incident along $[0001]_{Zno}$ and $[1\bar{1}00]_{ZnO}$, respectively. The upper RHEED patterns in (a)–(f) were in situ taken at growth temperature, and lower ones were taken after cooling to room temperature in the PLD chamber. The line profile shown in the bottom right corner is plotted from AFM image in (a). (For interpretation of the reference to color in this figure legend, the reader is referred to the web version of this article.)

films grown on *r*-plane sapphire. Due to large anisotropic lattice and thermal mismatches in two in-plane directions [36,38], the surface may reconstruct during cooling. In addition, the surface roughness of ZnO increases with further growth. The roughness is ~0.33 nm for 1200 pulses LT-ZnO, and it increases to ~0.60 nm after 2400 pulses deposition and ~1.2 nm for 180 nm thick film. Also, the grains emerge as elongated islands with ~30–80 nm width and ~60–160 nm length for 2400-pulse LT-ZnO. These elongated grains gradually extend to form stripes in *c*-direction. As shown in Fig. 2(d), large stripes in about 160–600 nm length and 60–160 nm width are formed by coalescence in both *c*- and *m*-directions. Each stripe actually consists of many sub-grains of 40–60 nm length, which make stripes of LT-ZnO rougher than those of HT-ZnO. However, straight streaks in RHEED are observed again along ZnO *c*-direction, suggesting that large stripes remain with relatively smooth surface.

In comparison with HT-ZnO which shows step morphology in initial growth, LT-ZnO islands form on the substrate in the beginning. It makes the surface of HT-ZnO are smoother than that of LT-ZnO. (0.1 nm for 200-pulse HT-ZnO vs. 0.17 nm for 100-pulse LT-ZnO) Both HT- and LT-ZnO should evolve into stripy morphologies with film thickness. However, the stripes of HT-ZnO are straight

with 0.3–1.2 nm height difference, whereas LT-ZnO stripes consist of many sub-grains in 2–4.5 nm height variation. Also, LT-ZnO shows rougher surface than HT-ZnO in similar thickness (for example, roughness 0.96 nm versus 0.41 nm for similar film thickness in ∼200 nm).

From the above RHEED and AFM observations, it is evident that HT-ZnO and LT-ZnO have different growth mode in the early stage, but both eventually develop to similar stripe morphology for films thicker than 100 nm. Kametani et al. have studied that the initial nucleation of ZnO nanodots on stepped *a*-, *c*- and *r*-plane sapphire substrates at 600 °C [39]. The dots were formed not only on the terraces but also on the step edges of sapphire; however, the dots on *r*-plane sapphire preferred to align on the step edges due to smaller number of dangling bonds on *r*-plane sapphire surface than *a*- and *c*-plane ones. As a result, there may have a larger diffusion length on *r*-plane sapphire. Because the diffusion length is also temperature-dependent, the distinction of the morphology in the early stage of ZnO growth at high temperature from that at low temperature can be rationalized. For further growth of ZnO, anisotropic growth characteristics due to anisotropic growth and surface diffusion rates caused by its structural asymmetry of ZnO *a*-plane [37,40] my play a predominate role on the development of film surface morphologies which therefore evolves into stripy morphology for both HT- and LT-ZnO.

4. Conclusions

In summary, distinct growth morphology developed in the early stage of *a*-plane ZnO growth on *r*-plane sapphire has been observed at 750 °C for HT-ZnO and 450 °C for LT-ZnO. HT-ZnO shows step morphology for initial growth, while LT-ZnO exhibits island growth in the very early stage. Cooling from growth temperature to room temperature may result in the change of surface morphology as illustrated in in situ RHEED patterns. For thick film growth over 100 nm, both HT-ZnO and LT-ZnO films evolve into similar stripe morphology.

Acknowledgment

This research was partially supported by National Science Council, Taiwan, R.O.C. under contract number of NSC98-2221-E-009-042-MY3.

References

[1] T. Aoki, Y. Hatanaka, D.C. Look, Applied Physics Letters 76 (2000) 3257.
[2] X.-L. Guo, J.-H. Choi, H. Tabata, T. Kawai, Japanese Journal of Applied Physics 40 (2001) L177.
[3] A. Tsukazaki, M. Kubota, A. Ohtomo, T. Onuma, K. Ohtani, H. Ohno, S.F. Chichibu, M. Kawasaki, Japanese Journal of Applied Physics 44 (2005) L643.
[4] Y. Ryu, T.-S. Lee, J.A. Lubguban, H.W. White, B.-J. Kim, T.-S. Park, C.-J. Youn, Applied Physics Letters 88 (2006) 241108.
[5] K. Nomura, H. Ohta, A. Takagi, T. Kamiya, M. Hirano, H. Hosono, Nature 432 (2004) 488.
[6] H.Q. Chiang, J.F. Wager, R.L. Hoffman, J. Jeong, D.A. Keszler, Applied Physics Letters 86 (2005) 013503.
[7] L.S. Hung, C.H. Chen, Materials Science & Engineering R: Reports 39 (2002) 143.
[8] X. Jiang, F.L. Wong, M.K. Fung, S.T. Lee, Applied Physics Letters 83 (2003) 1875.
[9] S.-H.K. Park, J.-I. Lee, C.-S. Hwang, H.Y. Chu, Japanese Journal of Applied Physics 44 (2005) L242.
[10] B. Rech, H. Wagner, Applied Physics A: Materials Science & Processing 69 (1999) 155.
[11] K. Ramanathan, M.A. Contreras, C.L. Perkins, S. Asher, F.S. Hasoon, J. Keane, D. Young, M. Romero, W. Metzger, R. Noufi, J. Ward, A. Duda, Progress in Photovoltaics: Research and Applications 11 (2003) 225.
[12] R. Klenk, J. Klaer, R. Scheer, M.C. Lux-Steiner, I. Luck, N. Meyer, U. Rühle, Thin Solid Films 480–481 (2005) 509.
[13] P. Waltereit, O. Brandt, A. Trampert, H.T. Grahn, J. Menniger, M. Ramsteiner, M. Reiche, K.H. Ploog, Nature 406 (2000) 865.
[14] T. Makino, A. Ohtomo, C.H. Chia, Y. Segawa, H. Koinuma, M. Kawasaki, Physica E 21 (2004) 671.
[15] T. Makino, Y. Segawa, M. Kawasaki, H. Koinuma, Semiconductor Science and Technology 20 (2005) S78.
[16] X. Li, X. Ni, J. Lee, M. Wu, Ü. Özgür, H. Morkoc, T. Paskova, G. Mulholand, K.R. Evans, Applied Physics Letters 95 (2009) 121107.
[17] J.H. Son, J.L. Lee, Applied Physics Letters 97 (2010) 032109.
[18] S.P. Chang, T.C. Lu, L.F. Zhuo, C.Y. Jang, D.W. Lin, H.C. Yang, H.C. Kuo, S.C. Wang, Journal of the Electrochemical Society 157 (2010) H501.
[19] X.Q. Lv, J.Y. Zhang, W.J. Liu, X.L. Hu, M. Chen, B.P. Zhang, Journal of Physics D: Applied Physics 44 (2011) 365401.
[20] M. Lange, C.P. Dietrich, L. Brachwitz, M. Stölzel, M. Lorenz, M. Grundmann, Physica Status Solidi (RRL) 6 (2012) 31.
[21] M. Brandt, M. Lange, M. Stölzel, A. Müller, G. Benndorf, J. Zippel, J. Lenzner, M. Lorenz, M. Grundman, Applied Physics Letters 97 (2010) 052101.
[22] F. Bernardini, V. Fiorentini, D. Vanderbilt, Physical Review B 56 (1997) R10024.
[23] J. Narayan, B.C. Larson, Journal of Applied Physics 93 (2003) 278.
[24] V. Srikant, V. Sergo, D.R. Clarke, Journal of the American Ceramic Society 78 (1995) 1931.
[25] Y.J. Kim, Y.T. Kim, H.K. Yang, J.C. Park, J.I. Han, Y.E. Lee, H.J. Kim, Journal of Vacuum Science and Technology A 15 (1997) 1103.
[26] S.K. Han, S.K. Hong, J.W. Lee, J.Y. Lee, J.H. Song, Y.S. Nam, S.K. Chang, T. Minegishi, T. Yao, Journal of Crystal Growth 309 (2007) 121.
[27] S. Yamauchi, H. Handa, A. Nagayama, T. Hariu, Thin Solid Films 345 (1999) 12.
[28] Y. Liu, C.R. Gorla, S. Liang, N. Emanetoglu, Y. Lu, H. Shen, M. Wraback, Journal of Electronic Materials 29 (2000) 69.
[29] J.W. Lee, S.K. Han, S.K. Hong, J.Y. Lee, T. Yao, Journal of Crystal Growth 310 (2008) 4102.
[30] J.W. Lee, S.K. Han, S.K. Hong, J.Y. Lee, Applied Surface Science 256 (2010) 1849.
[31] J.M. Chauveau, C. Morhain, M. Teisseire, M. Laügt, C. Deparis, J. Zuniga-Perez, B. Vinter, Microelectronics Journal 40 (2009) 512.
[32] M. Karger, M. Schilling, Physical Review B 71 (2005) 075304.
[33] S.K. Han, H.S. Lee, D.S. Lim, S.-K. Hong, N. Yoon, D.-C. Oh, B.J. Ahn, J.-H. Song, T. Yao, Journal of Vacuum Science and Technology A 29 (2011), 03A111.
[34] J.-M. Chauveau, C. Morhain, B. Lo, B. Vinter, P. Vennéguès, M. Laügt, D. Buell, M. Tesseire-Doninelli, G. Neu, Applied Physics A 88 (2007) 65.
[35] C.-Y. Peng, J.-S. Tian, W.-L. Wang, Y.-T. Ho, S.-C. Chuang, Y.-H. Chu, L. Chang, Journal of Vacuum Science and Technology A 29 (2011), 03A110.
[36] C.-Y. Peng, Y.-A. Liu, W.-L. Wang, J.-S. Tian, L. Chang, Applied Physics Letters 101 (2012) 151907.
[37] T.C. Zhang, Z.X. Mei, A. Yu Kuznetsov, X.L. Du, Journal of Crystal Growth 325 (2011) 93.
[38] G. Saraf, Y. Lu, T. Siegrist, Applied Physics Letters 93 (2008) 041903.
[39] K. Kametani, H. Imamoto, S. Fujita, Physica E 32 (2006) 33.
[40] U. Diebold, L.V. Koplitz, O. Dulub, Applied Surface Science 237 (2004) 336.